Land Use and Land Cover Change Analysis Following the 2025 Myanmar Earthquake

Kanai, S. [1*], Owa, R.[2], Ye, H.[3] and Kozan, O.[4]

[1]Graduate School of Asian and African Area Studies, Kyoto University, Research Bldg. No.2 Yoshida-Honmachi, Sakyo-ku, Kyoto, Japan. kanai.shindai.76k@st.kyoto-u.ac.jp

[2]Graduate School of Asian and African Area Studies, Kyoto University, Research Bldg. No.2 Yoshida-Honmachi, Sakyo-ku, Kyoto, Japan. owa.rin.45x@st.kyoto-u.ac.jp

[3]Center for Southeast Asian Studies, Kyoto University, 46 Shimoadachi-cho, Yoshida, Sakyo-ku, Kyoto, Japan. yehtet@cseas.kyoto-u.ac.jp

[4]Center for Southeast Asian Studies, Kyoto University, 46 Shimoadachi-cho, Yoshida, Sakyo-ku, Kyoto, Japan. kozan@cseas.kyoto-u.ac.jp

Abstract: On March 28, 2025, two major earthquakes struck central Myanmar, severely affecting communities already weakened by ongoing armed conflict. This study assessed the impacts of the earthquake on land use and land cover (LULC) using remote sensing techniques. Sentinel-1 Synthetic Aperture Radar (SAR) and Sentinel-2 optical imagery were combined to generate pre- and post-earthquake LULC maps for Mandalay, one of the most affected regions. Ground-truth data were derived from the ESA WorldCover 2021 product and visually verified using Google Earth imagery. The classification employed a Random Forest algorithm implemented on Google Earth Engine, incorporating spectral indices, SAR backscatter, and topographic slope as features. Results showed high overall accuracy for the pre-earthquake classification, while changes between pre- and post-earthquake LULC were relatively minor, likely due to the localized nature of the seismic event and residual classification noise in cropland areas. Future work will focus on parcel-based analyses to better capture subtle land surface and socio-environmental changes.

Keywords: LULC, Earthquake Damage Assessment, Southeast Asian Area Studies

1. Introduction

On March 28, 2025, two major earthquakes with magnitudes of 7.7 and 6.4 struck central Myanmar. The country has been experiencing continuous armed conflict since the military coup in 2021, and the earthquakes further exacerbated the already fragile conditions of many communities. More than 3,400 deaths and approximately 40,000 damaged buildings have been reported so far (Phattharapornjaroen, et al. 2025).

This study aims to assess the impacts of the 2025 Myanmar earthquake using remote sensing techniques, particularly in areas where field surveys are difficult to conduct due to ongoing conflict. To achieve this, we generated land use and land cover (LULC) maps before and after the earthquake. Land use refers to human activities and management of land, while land cover represents the physical characteristics of the Earth's surface. By visualizing the spatial patterns of land use and land cover, we seek to understand how both environmental and socio-economic

landscapes changed following the earthquake. For the creation of the LULC maps, optical Sentinel-2 and Synthetic Aperture Radar (SAR) Sentinel-1 satellite data were employed. The study area focuses on Mandalay in central Myanmar, which was among the most severely affected regions near the earthquake's epicenter.

2. Methodology

2.1 Ground-truth collection

Accurate ground-truth data are essential for supervised land use and land cover (LULC) classification, as they serve as training and validation samples. To efficiently obtain reliable reference data without conducting field surveys in conflict-affected areas, this study utilized the global LULC dataset ESA WorldCover 2021, produced by the European Space Agency (ESA). The WorldCover product provides global 10 m resolution classification with an overall accuracy of approximately 74.4% (ZanagaF et al., 2021), making it suitable as a baseline reference for regional-scale analyses.

Five LULC classes were defined in this study: Water, Forest, Cropland, Built-up, and Bareland. For each corresponding WorldCover category, 200 random points were initially sampled as ground-truth candidates. Each point was visually inspected using high-resolution Google Earth imagery to remove misclassified pixels or those located on class boundaries. After visual verification, the final set of ground-truth points consisted of Water (n = 150), Forest (n = 153), Cropland (n = 126), Built-up (n = 106), and Bareland (n = 66). These samples were subsequently used for both training and accuracy assessment of the LULC classification.

2.2 Satellite data processing and feature generation

This study utilized both Sentinel-2 optical imagery and Sentinel-1 Synthetic Aperture Radar (SAR) data. By combining optical and radar datasets, we aimed to increase the diversity of input features and improve classification accuracy. For each dataset, median composite images were generated for two temporal periods before (2024) and after (2025) the earthquake. The compositing periods were set to March 29 – May 31 and June 1 – September 30, respectively. Using two seasonal composites allowed for the inclusion of phenological variations and improved discrimination among LULC classes.

For Sentinel-2, cloud-affected pixels were masked using the S2 Cloud Probability product by retaining only pixels with a cloud probability below 60%. Several spectral indices were then derived to enhance class separability:

NDVI (Normalized Difference Vegetation Index) = (NIR – Red) / (NIR + Red)
GRVI (Green-Red Vegetation Index) = (Green – Red) / (Green + Red)
NDBI (Normalized Difference Built-up Index) = (SWIR – NIR) / (SWIR + NIR)
NDWI (Normalized Difference Water Index) = (Green – NIR) / (Green + NIR)
NDMI (Normalized Difference Moisture Index) = (NIR – SWIR) / (NIR + SWIR)

TGSI (Triangular Greenness and Soil Index) = (Green – Red) / (Green + Red – Blue)

In addition to spectral and radar information, topographic data were incorporated. Slope was calculated from the AW3D Digital Elevation Model (DEM) provided by the Japan Aerospace Exploration Agency (JAXA) and used as an additional feature (Tadono et al. 2015).

The complete list of features used for classification is summarized in Table 1.

Table 1: All feature values used for this research.

	Satellite	Feature
1	Sentinel-2	B2
2	Sentinel-2	B3
3	Sentinel-2	B4
4	Sentinel-2	B8
5	Sentinel-2	B11
6	Sentinel-2	B12
7	Sentinel-2	NDVI
8	Sentinel-2	NGRVI
9	Sentinel-2	NDBI
10	Sentinel-2	NDWI
11	Sentinel-2	NDMI
12	Sentinel-2	TGSI
13	Sentinel-1	VV
14	Sentinel-1	VH
15	(AW3D)	Slope

2.3 Classification and accuracy assessment

For the LULC classification, we employed the Random Forest (RF) algorithm, which has been widely recognized for its robustness and effectiveness in remote sensing–based land cover mapping. The classification was performed on Google Earth Engine (GEE) using the smileRandomForest classifier. The number of trees (numberOfTrees) was set to 200, while all other parameters were kept at their default values. Because the Sentinel-2 imagery occasionally contained NoData pixels due to cloud masking, those pixels were classified using only the Sentinel-1 SAR backscatter values (HH and HV polarizations).

The ground-truth dataset described in Section 2.1 was randomly divided into 70% for training and 30% for testing for each LULC class. The testing subset was not used during model training; it was solely used for evaluating the classification accuracy. Based on the testing data, a confusion matrix was generated to assess the classification performance for the pre-earthquake (2024) map.

3. Results

The results of the LULC classification for the Mandalay region of Myanmar are presented in Figures 1. The confusion matrix based on the pre-earthquake (2024) classification is shown in Table

2. Overall, the classification achieved high accuracy, demonstrating the reliability of the combined Sentinel-1 and Sentinel-2–based approach.

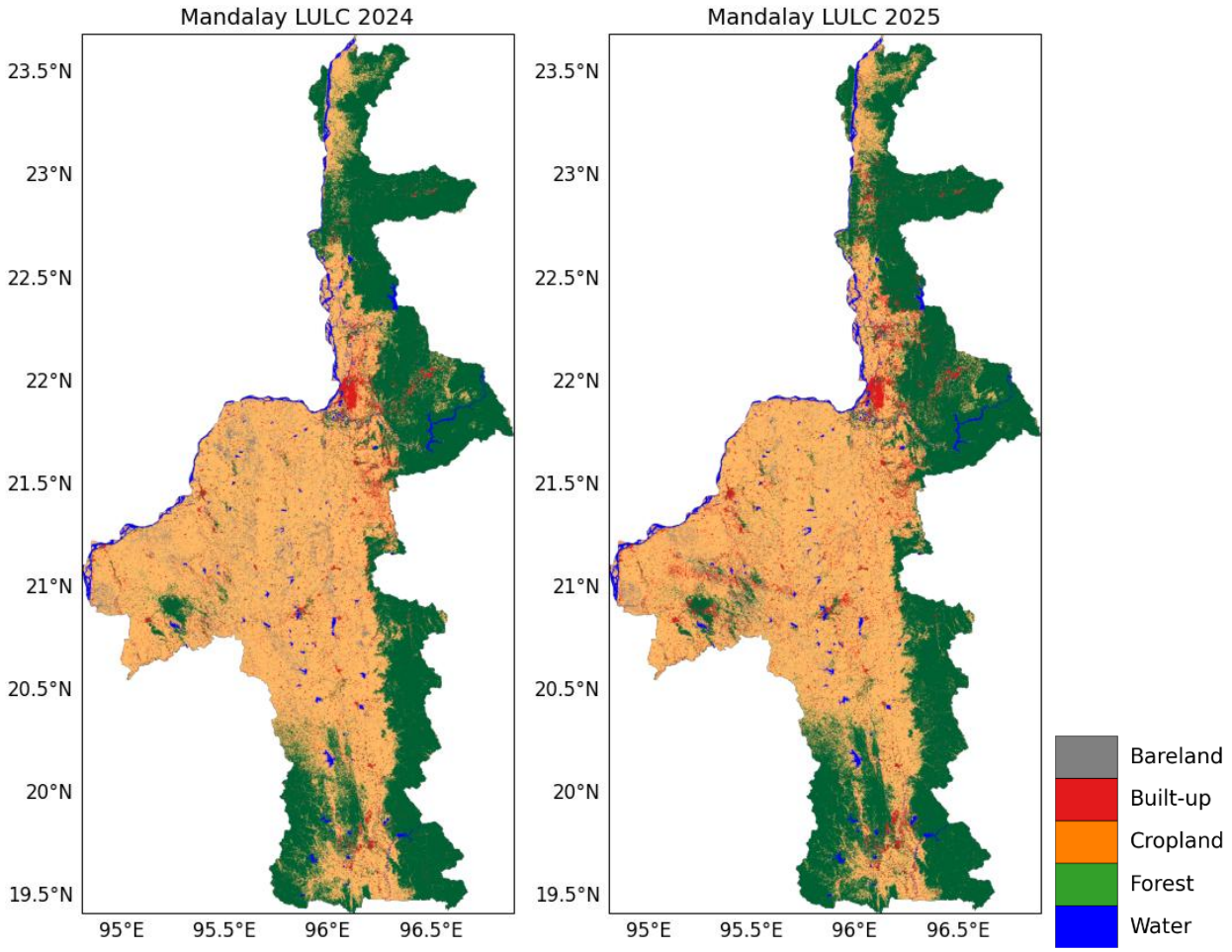

Figure 1: LULC maps of pre/post earthquake

Table 2: Confusion matrix of Mandalay LULC 2024 (pre-earthquake)

		Validation						User's accuracy (%)
		Water	Forest	Croopland	Built-up	Bareland	Total	
Classified	Water	**41**	0	0	0	0	41	**100.00**
	Forest	0	**48**	4	0	0	52	**92.31**
	Cropland	1	0	**30**	0	1	32	**93.75**
	Built-up	0	0	5	**34**	1	40	**85.00**
	Bareland	2	0	0	0	**13**	15	**86.67**
	Total	44	48	39	34	15	**180**	---
Producer's Accuracy (%)		**93.18**	**100.00**	**76.92**	**100.00**	**86.67**	---	**Overall accuracy (%) 92.22**

4. Conclusion

The overall LULC changes observed between the pre- and post-earthquake periods were relatively minor. Two main factors likely explain this outcome. First, the 2025 Myanmar earthquake was a shallow inland event rather than a tsunami-generating or nuclear-related disaster, and therefore did not induce large-scale land cover transformation or displacement of populations. Second, the Cropland class exhibited relatively high misclassification rates, which may have masked small-scale changes in Built-up areas that were actually affected by the earthquake.

Considering these limitations, future work will focus on implementing a parcel-based classification approach to analyze how spectral and radar features within each land parcel change before and after the earthquake. Such an approach is expected to better capture subtle LULC dynamics in built-up and agricultural regions.

References

Phattharapornjaroen, P., Burivong, R., and Khorram-Manesh, A. 2025, Myanmar Earthquake Aftermarth – Critical Update and Expanded Analysis, *Disaster Medicine and Public Health Preparedness*, 19, e125, pp. 1-7.

D. Zanaga, R. Van De Kerchove, D. Daems, et al.,2022. ESA World-Cover 10 m 2021 v200, *Zenodo*

Tadono, T., Junichi, T., Tsutsui, K., Oda, F., and Nagai, H., 2015. Status of 'ALOS World 3D (AW3D)' Global DSM Generation. *2015 IEEE International Geoscience and Remote Sensing Symposium (IGARSS)*, 3822–25. IEEE.